Contact Interactions, Large Extra Dimensions and Leptoquarks at THERA

Aleksander Filip Żarnecki
Institute of Experimental Physics, Warsaw University,
Hoża 69, 00-681 Warszawa, Poland
E-mail: zarnecki@fuw.edu.pl

May 24, 2001

arXiv:hep-ph/0104107 11 Apr 2001

Abstract

The sensitivity of THERA to different models of "new physics" has been studied, both for the contact interaction approximation and for the resonance production. For contact interaction models conserving parity, scales up to about 18 TeV can be explored at THERA, extending considerably beyond the existing bounds. Significant improvement of existing limits is also expected for models with large extra dimensions. Effective Plank mass scales up to about 2.8 TeV can be probed. THERA will be the best machine to study leptoquark properties, for leptoquark masses up to about 1 TeV. It will be sensitive to the leptoquark Yukawa couplings down to $\lambda_{LQ} \sim 10^{-2}$.

1 Introduction

Search for "new physics" has always been one of the most important subjects in the field of particle physics. Possibility of discovering new particles, new interactions and/or other new phenomena is always considered as a main argument for building new, more powerful colliders. Collected in this paper are results concerning possible "new physics" searches at THERA, prepared as a part of the dedicated THERA physics study. The collider project and running options are briefly summarized in Sect. 2. Models considered in this paper are introduced in Sect. 3. The method used for the analysis has been developed for the global analysis of the existing data [1, 2] and is briefly described in Sect. 4. Some of the results discussed in Sect. 5 have been already presented in [3].

2 THERA collider

THERA has been proposed as the next generation *ep* collider, a straightforward extension of the TESLA project. It would bring high-energy electrons or positrons from the linear

accelerator into collisions with high-energy protons from the existing HERA collider. Using both arms of TESLA center-of-mass energies of up to 1.6 TeV could be obtained at THERA, exceeding the energy range currently accessible at HERA by up to a factor of five.

Following THERA running scenarios are considered in this paper:

- For nominal electron beam energy of E_e=250 GeV and proton beam energy of E_p=1000 GeV integrated luminosity of about 40 pb^{-1} is expected in a year. Results presented for this option assume integrated luminosity of 100 pb^{-1} for e^-p and/or 100 pb^{-1} for e^+p collisions. It will be referred to as THERA-250.

- Using both arms of TESLA, electron beam energy can be increased to E_e=500 GeV. Assumed integrated luminosity for this scenario is also 100 pb^{-1} for e^-p and/or 100 pb^{-1} for e^+p collisions. It will be referred to as THERA-500.

- With TESLA machine upgraded in power, electron energies as high as E_e=800 GeV are possible for THERA operation. In this case proton beam energy is lowered to E_p=800 GeV, to provide maximum luminosity. Results presented for this option assume integrated luminosity of 200 pb^{-1} for e^-p and/or 200 pb^{-1} for e^+p collisions. It will be referred to as THERA-800.

3 Models of new physics

3.1 Contact Interactions

Four-fermion contact interactions are an effective theory, which allows us to describe, in the most general way, possible low energy effects coming from "new physics" at much higher energy scales. As very strong limits have been already placed on both scalar and tensor contact interactions [4], only vector contact interactions are considered in this analysis. The influence of the vector contact interactions on the ep NC DIS cross-section can be described as an additional term in the tree level $eq \to eq$ scattering amplitude [5, 6]:

$$M^{e_i q_j \to e_i q_j}(t) \;=\; -\frac{4\pi\alpha_{em} e_q}{t} \;+\; \frac{4\pi\alpha_{em}}{sin^2\theta_W \cdot cos^2\theta_W} \cdot \frac{g_i^e g_j^q}{t - M_Z^2} \;+\; \eta_{ij}^{eq} \qquad (1)$$

where $t = -Q^2$ is the Mandelstam variable describing the four-momentum transfer between the electron and the quark, e_q is the electric charge of the quark in units of the elementary charge, the subscripts i and j label the chiralities of the initial lepton and quark respectively ($i, j = L, R$), g_i^e and g_j^q are electroweak couplings of the electron and the quark, and η_{ij}^{eq} are the contact interaction couplings.

In the most general case, vector contact interactions are described by 4 independent couplings for every quark flavor. As ep scattering is sensitive predominantly to electron-up and electron-down quark couplings, 8 independent couplings should be considered. However, it is not be possible, in one experiment, to put significant constraints on all

of these couplings simultaneously, without additional assumptions. Therefor, only one-parameter models, assuming fixed relations between the separate couplings, are considered in this paper. Relations between couplings assumed for different models are presented in Tab. 1 and 2. Listed in Tab. 1 are models with defined coupling chirality. Models in Tab. 2 fulfill the relation

$$\eta^{eq}_{LL} + \eta^{eq}_{LR} - \eta^{eq}_{RL} - \eta^{eq}_{RR} \;=\; 0$$

which is imposed to conserve parity, and to avoid strong limits coming from atomic parity violation measurements. In the presented contact interaction analysis it is also assumed that all up type and down type quarks have the same contact interaction couplings:

$$\begin{aligned} \eta^{eu}_{ij} &= \eta^{ec}_{ij} = \eta^{et}_{ij} \\ \eta^{ed}_{ij} &= \eta^{es}_{ij} = \eta^{eb}_{ij} \end{aligned}$$

Coupling η can be related to the effective mass scale of contact interactions Λ:

$$\eta \;=\; \pm\frac{g^2_{CI}}{\Lambda^2}$$

where the coupling strength of new interactions is by convention set to $g_{CI} = \sqrt{4\pi}$.

3.2 Large Extra Dimensions

Model proposed by Arkani-Hamed, Dimopoulos and Dvali [7, 8] assumes the space-time is $4+n$ dimensional. Standard Model particles, including strong and electroweak bosons are confined to 4 dimensions, but the gravity can propagate in the extra dimensions as well. With very large extra dimensions, the effective Plank scale M_S can be of the order of TeV. The graviton, after summing the effects of its excitations in the extra dimensions, couples to the Standard Model particles with an effective strength of $1/M_S$. At high energies, gravitation interaction can become comparable in strength to electroweak interactions. Virtual graviton exchange contribution to $eq \to eq$ scattering can be described by an effective contact interactions. Contribution to the scattering amplitude (1), equivalent to the cross-section formula given in [9], can be written as:

$$\begin{aligned} \eta^{eq}_{LL} \;=\; \eta^{eq}_{RR} \;&=\; -\frac{\pi\lambda}{2M_S^4}\,(4t+s) \\ \eta^{eq}_{LR} \;=\; \eta^{eq}_{RL} \;&=\; -\frac{\pi\lambda}{2M_S^4}\,(4t+3s) \end{aligned}$$

where t and s are the Mandelstam variables describing electron-quark scattering. By convention the coupling strength is set to $\lambda = \pm 1$.

3.3 Leptoquarks

In this paper a general classification of leptoquark states proposed by Buchmüller, Rückl and Wyler [10] will be used. The Buchmüller-Rückl-Wyler (BRW) model is based on the

Model	η^{ed}_{LL}	η^{ed}_{LR}	η^{ed}_{RL}	η^{ed}_{RR}	η^{eu}_{LL}	η^{eu}_{LR}	η^{eu}_{RL}	η^{eu}_{RR}
q_{LL}	$+\eta$				$+\eta$			
q_{LR}		$+\eta$				$+\eta$		
q_{RL}			$+\eta$				$+\eta$	
q_{RR}				$+\eta$				$+\eta$
d_{LL}	$+\eta$							
d_{LR}		$+\eta$						
d_{RL}			$+\eta$					
d_{RR}				$+\eta$				
u_{LL}					$+\eta$			
u_{LR}						$+\eta$		
u_{RL}							$+\eta$	
u_{RR}								$+\eta$

Table 1: Relations between couplings for contact interaction models with defined coupling chirality considered in this paper.

Model	η^{ed}_{LL}	η^{ed}_{LR}	η^{ed}_{RL}	η^{ed}_{RR}	η^{eu}_{LL}	η^{eu}_{LR}	η^{eu}_{RL}	η^{eu}_{RR}
VV	$+\eta$	$+\eta$	$+\eta$	$+\eta$	$+\eta$	$+\eta$	$+\eta$	$+\eta$
AA	$+\eta$	$-\eta$	$-\eta$	$+\eta$	$+\eta$	$-\eta$	$-\eta$	$+\eta$
VA	$+\eta$	$-\eta$	$+\eta$	$-\eta$	$+\eta$	$-\eta$	$+\eta$	$-\eta$
X1	$+\eta$	$-\eta$			$+\eta$	$-\eta$		
X2	$+\eta$		$+\eta$		$+\eta$		$+\eta$	
X3	$+\eta$			$+\eta$	$+\eta$			$+\eta$
X4		$+\eta$	$+\eta$			$+\eta$	$+\eta$	
X5		$+\eta$		$+\eta$		$+\eta$		$+\eta$
X6			$+\eta$	$-\eta$			$+\eta$	$-\eta$
U1					$+\eta$	$-\eta$		
U2					$+\eta$		$+\eta$	
U3					$+\eta$			$+\eta$
U4						$+\eta$	$+\eta$	
U5						$+\eta$		$+\eta$
U6							$+\eta$	$-\eta$

Table 2: Relations between couplings for the parity conserving contact interaction models considered in this paper.

assumption that new interactions should respect the $SU(3)_C \times SU(2)_L \times U(1)_Y$ symmetry of the Standard Model. In addition leptoquark couplings are assumed to be family diagonal (to avoid FCNC processes) and to conserve lepton and baryon numbers (to avoid rapid proton decay). Taking into account very strong bounds from rare decays [11] it is also assumed that leptoquarks couple either to left- or to right-handed leptons. With all these assumptions there are 14 possible states (isospin singlets or multiplets) of scalar and vector leptoquarks. Table 3 lists these states according to the so-called Aachen notation [12]. An S(V) denotes a scalar(vector) leptoquark and the subscript denotes the weak isospin. When the leptoquark can couple to both right- and left-handed leptons, an additional superscript indicates the lepton chirality. A tilde is introduced to differentiate between leptoquarks with different hypercharge. Listed in Tab. 3 are the leptoquark fermion number F, electric charge Q, and the branching ratio to an electron-quark pair (or electron-antiquark pair), β. The leptoquark branching fractions are predicted by the BRW model and are either 1, $\frac{1}{2}$ or 0. For a given electron-quark branching ratio β, the branching ratio to the neutrino-quark is by definition $(1-\beta)$. Also included in Tab. 3 are the flavours and chiralities of the lepton-quark pairs coupling to a given leptoquark type. In three cases the squark flavours (in supersymmetric theories with broken R-parity) with corresponding couplings are also indicated. Present analysis takes into account only leptoquarks which couple to the first-generation leptons (e, ν_e) and first-generation quarks (u, d). It is also assumed that one of the leptoquark types gives the dominant contribution, as compared with other leptoquark states and that the interference between different leptoquark states can be neglected. Using this simplifying assumption, different leptoquark types can be considered separately. Finally, it is assumed that different leptoquark states within isospin doublets and triplets have the same mass.

In the limit of heavy leptoquark masses ($M_{LQ} \gg \sqrt{s}$) the effect of leptoquark production or exchange is equivalent to a vector type $eeqq$ contact interaction. Contribution to the $eq \to eq$ scattering amplitude (1) does not depend on the process kinematics and can be written as

$$\eta_{ij}^{eq} \;=\; a_{ij}^{eq} \cdot \left(\frac{\lambda_{LQ}}{M_{LQ}}\right)^2 \quad ,$$

where M_{LQ} is the leptoquark mass, λ_{LQ} the leptoquark-electron-quark Yukawa coupling and the coefficients a_{ij}^{eq} are given in Tab. 4 [13].

For leptoquark masses comparable with the available ep center-of-mass energy u-channel leptoquark exchange process and the s-channel leptoquark production have to be considered separately. Corresponding diagrams for F=0 and F=2 leptoquarks are shown in Fig. 1. The leptoquark contribution to the scattering amplitude can be now described by the following formulae:

- for u-channel leptoquark exchange (F=0 leptoquark in e^-q or $e^+\bar{q}$ scattering, or $|F|$=2 leptoquark in e^+q or $e^-\bar{q}$ scattering)

$$\eta_{ij}^{eq}(s,u) \;=\; \frac{a_{ij}^{eq} \cdot \lambda_{LQ}^2}{M_{LQ}^2 - u} \quad ,$$

Model	Fermion number F	Charge Q	$BR(LQ \to e^{\pm} q)$ β	Coupling		Squark type
$S_\circ^L$	2	$-1/3$	1/2	$e_L u$	νd	$\tilde{d_R}$
$S_\circ^R$	2	$-1/3$	1	$e_R u$		
$\tilde{S}_\circ$	2	$-4/3$	1	$e_R d$		
$S_{1/2}^L$	0	$-5/3$	1	$e_L \bar{u}$		
		$-2/3$	0		$\nu \bar{u}$	
$S_{1/2}^R$	0	$-5/3$	1	$e_R \bar{u}$		
		$-2/3$	1	$e_R \bar{d}$		
$\tilde{S}_{1/2}$	0	$-2/3$	1	$e_L \bar{d}$		$\overline{\tilde{u}_L}$
		$+1/3$	0		$\nu \bar{d}$	$\overline{\tilde{d}_L}$
S_1	2	$-4/3$	1	$e_L d$		
		$-1/3$	1/2	$e_L u$	νd	
		$+2/3$	0		νu	
$V_\circ^L$	0	$-2/3$	1/2	$e_L \bar{d}$	$\nu \bar{u}$	
$V_\circ^R$	0	$-2/3$	1	$e_R \bar{d}$		
$\tilde{V}_\circ$	0	$-5/3$	1	$e_R \bar{u}$		
$V_{1/2}^L$	2	$-4/3$	1	$e_L d$		
		$-1/3$	0		νd	
$V_{1/2}^R$	2	$-4/3$	1	$e_R d$		
		$-1/3$	1	$e_R u$		
$\tilde{V}_{1/2}$	2	$-1/3$	1	$e_L u$		
		$+2/3$	0		νu	
V_1	0	$-5/3$	1	$e_L \bar{u}$		
		$-2/3$	1/2	$e_L \bar{d}$	$\nu \bar{u}$	
		$+1/3$	0		$\nu \bar{d}$	

Table 3: A general classification of leptoquark states in the Buchmüller-Rückl-Wyler model. Listed are the leptoquark fermion number, F, electric charge, Q (in units of elementary charge), the branching ratio to electron-quark (or electron-antiquark), β and the flavours of the coupled lepton-quark pairs. Also shown are possible squark assignments to the leptoquark states in the minimal supersymmetric theories with broken R-parity.

Model	a_{LL}^{ed}	a_{LR}^{ed}	a_{RL}^{ed}	a_{RR}^{ed}	a_{LL}^{eu}	a_{LR}^{eu}	a_{RL}^{eu}	a_{RR}^{eu}
$S_\circ^L$					$+\frac{1}{2}$			
$S_\circ^R$								$+\frac{1}{2}$
$\tilde{S}_\circ$				$+\frac{1}{2}$				
$S_{1/2}^L$						$-\frac{1}{2}$		
$S_{1/2}^R$			$-\frac{1}{2}$				$-\frac{1}{2}$	
$\tilde{S}_{1/2}$		$-\frac{1}{2}$						
S_1	$+1$				$+\frac{1}{2}$			
$V_\circ^L$	-1							
$V_\circ^R$				-1				
$\tilde{V}_\circ$								-1
$V_{1/2}^L$		$+1$						
$V_{1/2}^R$			$+1$				$+1$	
$\tilde{V}_{1/2}$						$+1$		
V_1	-1				-2			

Table 4: Coefficients a_{ij}^{eq} defining the effective contact interaction couplings $\eta_{ij}^{eq} = a_{ij}^{eq} \cdot \frac{\lambda_{LQ}^2}{M_{LQ}^2}$ for different models of scalar (upper part of the table) and vector (lower part) leptoquarks. Empty places in the table correspond to $a_{ij}^{eq} = 0$.

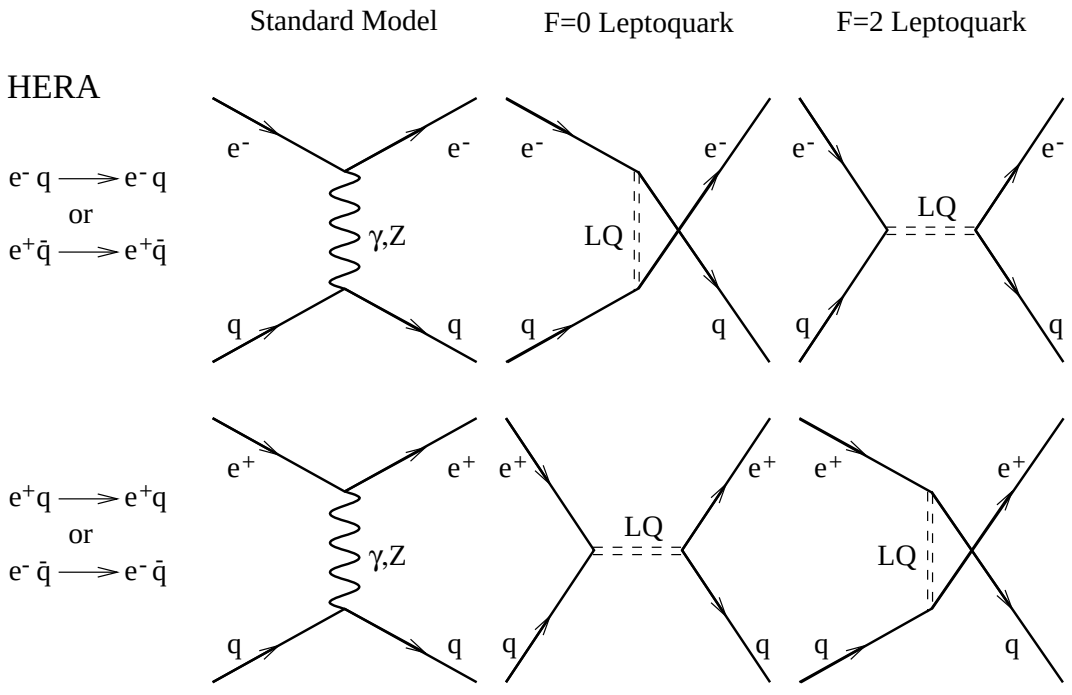

Figure 1: Diagrams describing leading order Standard Model processes and leptoquark contributions coming from F=0 and F=2 leptoquarks, for NC $e^{\pm}p$ DIS at THERA.

- for s-channel leptoquark production (F=0 leptoquark in e^+q or $e^-\bar{q}$ scattering, or $|F|$=2 leptoquark in e^-q or $e^+\bar{q}$ scattering)

$$\eta_{ij}^{eq}(s,u) \;=\; \frac{a_{ij}^{eq}\cdot\lambda_{LQ}^2}{M_{LQ}^2 - s - is\frac{\Gamma_{LQ}}{M_{LQ}}} \;\;,$$

where Γ_{LQ} is the total leptoquark width. The partial decay width for every decay channel is given by the formula:

$$\Gamma_{LQ} \;=\; \frac{\lambda_{LQ}^2 M_{LQ}}{8\pi(J+2)} \;\;,$$

where J is the leptoquark spin.

For leptoquark masses smaller than the available ep center-of-mass energy direct production of single leptoquarks can be considered. In the narrow-width approximation, the cross-section for single $F = 2$ leptoquark production in electron-proton scattering (via the electron-quark fusion) is given by:

$$\sigma^{ep\to LQ\;X}(M_{LQ},\lambda_{LQ}) \;=\; (J+1)\cdot\frac{\pi\lambda_{LQ}^2}{4M_{LQ}^2}\cdot x_{LQ}q(x_{LQ},M_{LQ}^2) \qquad (2)$$

where $q(x,Q^2)$ is the quark momentum distribution in the proton and $x_{LQ} = \frac{M_{LQ}^2}{s}$.

4 Analysis method

The analysis method used has been described in details in the recently published papers [1, 2]. For all models considered, limits on the model parameters can be extracted from the measured Q^2 distribution of NC DIS events at THERA. The leading-order doubly-differential cross-section for electron-proton NC DIS ($e^-p \to e^-X$) can be written as

$$\begin{aligned}\frac{d^2\sigma^{LO}}{dxdQ^2} \;=\; \frac{1}{16\pi}\sum_q \;& q(x,Q^2)\left\{|M_{LL}^{eq}|^2 + |M_{RR}^{eq}|^2(1-y)^2\left[|M_{LR}^{eq}|^2 + |M_{RL}^{eq}|^2\right]\right\} \;+ \\ & \bar{q}(x,Q^2)\left\{|M_{LR}^{eq}|^2 + |M_{RL}^{eq}|^2(1-y)^2\left[|M_{LL}^{eq}|^2 + |M_{RR}^{eq}|^2\right]\right\} \;\;,\end{aligned}$$

where x is the Bjorken variable, describing the fraction of the proton momentum carried by the struck quark (antiquark), $q(x,Q^2)$ and $\bar{q}(x,Q^2)$ are the quark and antiquark momentum distribution functions in the proton and M_{ij}^{eq} are the scattering amplitudes of (1), which can include contributions from "new physics".

The cross-section integrated over the x and Q^2 range of an experimental Q^2 bin from Q_{min}^2 to Q_{max}^2 is

$$\sigma^{LO} \;=\; \int_{Q_{min}^2}^{Q_{max}^2} dQ^2 \int_{\frac{Q^2}{s\cdot ymax}}^{1} dx\;\frac{d^2\sigma^{LO}}{dxdQ^2} \qquad (3)$$

where y_{max} is an upper limit on the reconstructed Bjorken variable y, $y = \frac{Q^2}{x\,s}$. In the presented analysis this limit is set to y_{max}=0.95. Eq. 3 is used to calculate numbers of expected events in Q^2 bins. Expected limits on model parameters, from high-Q^2 NC $e^{\pm}p$ DIS at THERA, are calculated assuming that no deviations from the Standard Model predictions will be observed.

For every value of the model parameter η ($\pm 4\pi/\Lambda^2$ for the contact interaction models, $\pm 1/M_S^4$ for large extra dimensions, $(\lambda_{LQ}/M_{LQ})^2$ for leptoquark models in the high-mass limit[1]) the probability function describing the agreement between the model and the data is calculated:

$$\mathcal{P}(\eta) \;\sim\; \prod_i P_i(\eta)$$

The product runs over all Q^2 bins i (separately for e^-p and e^+p data). The probability P_i described by the Poisson distribution

$$P_i(\eta) \;\sim\; \frac{n(\eta)^N \cdot exp(-n(\eta))}{N!}, \tag{4}$$

where N and $n(\eta)$ are the measured and expected number of events in a given bin. This formula properly takes into account statistical errors in the measured event distributions. The systematic errors in the Standard Model expectations are assumed to be correlated to 100% between different Q^2 bins, and increase from 1% at Q^2=1000 GeV^2 to 5% at Q^2=100000 GeV^2. The method used to include systematic errors, as well as the migration corrections resulting from the assumed Q^2 measurement resolution of 5% are discussed in detail in [1].

To constraint leptoquark Yukawa coupling values, for leptoquark masses smaller than the available ep center-of-mass energy, direct production of single leptoquarks is also considered, as described by (2). Only the leptoquark signal in the electron-jet decay channel is taken into account. Expected signal from single leptoquark production, for given leptoquark mass M_{LQ} and Yukawa coupling λ_{LQ}, is compared with the observed number of events from the Standard Model background (NC DIS) in the $\pm$5% mass window. The background is suppressed by applying a cut on the Bjorken variable y, which is optimized for every leptoquark type as a function of the leptoquark mass. After the y cut is imposed, probability function $\mathcal{P}(\lambda_{LQ}, M_{LQ})$ is calculated from the Poisson distribution (4). As $\mathcal{P}$ is not a probability distribution, it does not satisfy any normalization condition. Instead it is convenient to rescale the probability function in such a way that for the Standard Model it has the value of 1:

$$\mathcal{P}(\eta = 0) \;=\; 1.$$

Using the probability function $\mathcal{P}(\eta)$ limits on the model parameters are calculated. Rejected are all models (parameter values) which result in

$$\mathcal{P}(\eta) \;<\; 0.05 \tag{5}$$

[1] For leptoquark masses comparable with the available center-of-mass energy, two parameter probability function $\mathcal{P}(\lambda_{LQ}, M_{LQ})$ is considered and limits on λ_{LQ} are calculated as a function of the leptoquark mass M_{LQ}.

This is taken as the definition of the 95% confidence level (CL) exclusion limit.[2] Exclusion limits presented in this paper are lower limits in case of mass scales Λ or M_S, leptoquark mass M_{LQ} or M_{LQ}/λ_{LQ}, and upper limits in case of λ_{LQ}. For leptoquark masses smaller than the available center-of-mass energy, both indirect (from $\frac{d\sigma}{dQ^2}$) and direct λ_{LQ} limits are calculated, and the stronger one is presented.

5 Results

95% CL exclusion limits on the contact interaction mass scales Λ^- and Λ^+ (for negative and positive coupling signs) expected from the measurement of high-Q^2 NC DIS cross-sections at THERA, are presented in Tab. 5 and 6. Results presented are the mean values from 1000 MC experiments. Poisson fluctuations in the observed numbers of events can result in the statistical fluctuations in the limit values of the order of 10-20%. Current limits from the global contact interaction analysis [14][3] and from the global analysis of existing data in the large extra dimensions (ED) model [9] are included for comparison.

For contact interaction models violating parity (models with defined coupling chirality; Tab. 5), current limits from global analysis are already of the order of 10-20 TeV. This is mainly due to very strong constraints from the atomic parity violation (APV) measurements in cesium [15, 16, 17]. THERA running with the nominal electron beam energy of 250 GeV (THERA-250) will be only sensitive to mass scales from about 3 to 9 TeV. With electron beam energy increased to 500 GeV (THERA-500), contact interaction mass scale limits improve on average by 20-30%. Another improvement by similar factor is observed when going from THERA-500 to THERA-800 option. Nevertheless, even for high electron beam energies (THERA-500 and THERA-800) improvement of existing limits will only be possible for selected models (mainly models coupling to the u quark only).

For contact interaction models conserving parity (Tab. 6), current limits from global analysis are, on average, lower than for parity violating models. At the same time THERA sensitivity increases. Already at THERA-250 mass scale limits can be improved for about half of the considered models, provided that both e^-p and e^+p data are collected. With increasing electron beam energy, most limits can be significantly improved. From combined e^-p and e^+p data at THERA-800 limits on the contact interaction mass scales up to about 18 TeV can be obtained.

[2] For Gaussian shape of the probability function, condition (5) corresponds to $\pm 2.45\sigma$ limit. Mass scale limits presented in this paper would increase by 10 to 15%, if the definition more commonly used in the literature is used: $\mathcal{P}(\eta) = 0.147$ corresponding to $\pm 1.96\sigma$. However, this definition assumes the Gaussian shape of the probability function, which is not always the case. Therefor definition (5) is used as more "conservative". Same limit setting method has been used in the global analysis of existing data [2, 14].

[3] Numerical limit values presented in this paper differ slightly from limits presented in [14]. They have been recalculated using data on $eeqq$ interactions only. Data from neutrino scattering experiments and from charged current processes, which can be included in the analysis when assuming $SU(2)_L \times U(1)_Y$ symmetry of new interactions, were not used. This is because some of the considered models violate $SU(2)$ invariance.

Model	Current limits [TeV]		Expected 95% CL exclusion limits [TeV]																	
			THERA-250						THERA-500						THERA-800					
			e^-p		e^+p		$e^\pm p$		e^-p		e^+p		$e^\pm p$		e^-p		e^+p		$e^\pm p$	
	Λ^-	Λ^+	Λ^-	Λ^+	Λ^-	Λ^+	Λ^-	Λ^+	Λ^-	Λ^+	Λ^-	Λ^+	Λ^-	Λ^+	Λ^-	Λ^+	Λ^-	Λ^+	Λ^-	Λ^+
d_{LL}	23.3	8.4	5.6	4.7	5.0	4.2	6.3	5.5	7.3	6.0	6.5	5.6	8.1	7.1	8.8	7.4	7.8	6.8	9.8	8.7
d_{LR}	19.6	7.5	3.2	2.9	4.8	3.9	4.9	4.0	4.1	3.7	6.0	5.0	6.1	5.1	4.9	4.4	7.3	6.0	7.5	6.1
d_{RL}	7.4	20.4	2.7	3.3	3.9	4.8	3.9	4.9	3.5	4.3	5.0	6.0	5.0	6.2	4.2	5.1	6.0	7.4	6.0	7.5
d_{RR}	8.8	17.5	4.6	3.5	4.0	3.0	4.9	3.6	5.8	4.5	5.2	3.8	6.3	4.7	7.0	5.3	6.2	4.5	7.6	5.6
u_{LL}	14.7	11.3	7.9	8.3	5.6	5.9	8.5	8.8	9.8	10.3	7.0	7.6	10.5	10.9	12.2	12.7	8.7	9.2	13.0	13.5
u_{LR}	16.9	7.8	3.1	3.8	4.9	7.1	5.1	7.3	3.9	4.9	6.0	8.7	6.2	8.9	4.6	5.8	7.4	10.9	7.6	11.0
u_{RL}	7.1	18.3	3.2	3.4	4.7	6.2	4.9	6.3	4.0	4.5	6.0	7.7	6.2	7.8	4.7	5.3	7.3	9.4	7.4	9.6
u_{RR}	7.0	21.2	6.3	7.3	4.4	5.3	6.8	7.8	7.6	9.1	5.6	6.8	8.4	9.7	9.6	11.3	6.8	8.3	10.4	11.9
q_{LL}	26.1	10.9	4.2	7.2	3.5	4.8	4.3	7.3	5.3	8.8	4.6	6.1	5.5	9.0	6.4	10.9	5.4	7.4	6.6	11.2
q_{LR}	25.8	10.6	3.5	4.0	4.9	7.1	5.0	7.2	4.5	5.2	6.3	8.7	6.4	8.8	5.3	6.2	7.6	10.7	7.7	10.9
q_{RL}	10.2	27.3	3.4	4.1	5.1	7.0	5.2	7.2	4.4	5.4	6.5	8.7	6.6	8.9	5.2	6.4	7.8	10.7	8.0	10.9
q_{RR}	10.3	27.1	4.4	7.0	3.5	5.0	4.5	7.3	5.6	8.7	4.5	6.3	5.8	9.0	6.8	10.7	5.4	7.7	7.0	11.1

Table 5: 95% CL exclusion limits on the contact interaction mass scales Λ^- and Λ^+ (for negative and positive coupling signs respectively) expected from the measurement of high-Q^2 NC DIS cross-sections at THERA, for different running scenarios, as indicated in the table. Limits from the global analysis of existing data [1, 14] are included for comparison.

Model	Current limits [TeV]		Expected 95% CL exclusion limits [TeV]																	
			THERA-250						THERA-500						THERA-800					
			e^-p		e^+p		$e^\pm p$		e^-p		e^+p		$e^\pm p$		e^-p		e^+p		$e^\pm p$	
	Λ^-	Λ^+	Λ^-	Λ^+	Λ^-	Λ^+	Λ^-	Λ^+	Λ^-	Λ^+	Λ^-	Λ^+	Λ^-	Λ^+	Λ^-	Λ^+	Λ^-	Λ^+	Λ^-	Λ^+
VV	8.3	14.5	7.6	9.9	7.2	10.3	9.8	11.9	8.7	12.3	8.5	12.5	11.3	14.6	11.3	15.2	10.6	15.6	14.4	18.1
AA	11.2	10.8	4.7	9.2	8.4	6.2	9.3	9.3	6.2	11.2	10.4	8.1	11.1	11.4	7.3	14.0	12.8	9.7	13.9	14.1
VA	5.8	6.3	6.3	6.7	7.3	7.2	7.7	7.7	8.2	8.5	9.3	9.1	9.8	9.9	9.7	10.3	11.3	11.0	11.8	11.9
$X1$	8.5	8.6	4.2	7.2	6.8	5.4	7.2	7.3	5.6	8.8	8.5	7.0	8.7	9.1	6.5	10.9	10.4	8.4	10.8	11.2
$X2$	6.7	10.8	4.5	7.6	5.2	7.8	6.1	9.0	5.7	9.5	6.7	9.6	7.4	11.1	6.9	11.6	8.1	11.9	9.2	13.6
$X3$	8.8	12.0	7.0	9.4	4.0	6.2	7.4	9.7	7.9	11.5	5.2	7.9	8.2	11.9	10.5	14.2	6.1	9.6	11.0	14.7
$X4$	6.2	10.0	4.0	5.0	5.9	9.1	6.1	9.2	5.2	6.6	7.5	11.1	7.7	11.3	6.1	7.8	9.1	13.7	9.2	13.9
$X5$	5.6	9.1	4.5	7.4	5.1	7.9	5.8	8.9	5.8	9.2	6.6	9.8	7.2	11.0	6.9	11.3	7.9	12.0	8.8	13.6
$X6$	6.8	5.4	6.9	4.4	5.5	6.7	7.1	6.9	8.6	5.7	7.1	8.4	9.0	8.6	10.5	6.8	8.6	10.3	10.9	10.5
$U1$	6.3	13.0	7.1	8.1	6.2	5.1	8.1	8.1	8.3	9.9	7.7	6.7	9.7	10.1	10.7	12.3	9.5	8.0	12.2	12.5
$U2$	7.3	15.6	8.1	8.5	6.6	7.9	9.1	9.7	9.9	10.6	8.1	9.9	11.1	12.1	12.3	13.1	10.0	12.1	13.8	14.9
$U3$	8.9	19.8	10.8	10.8	7.6	7.7	11.5	11.4	13.3	13.3	9.6	9.9	14.2	14.2	16.5	16.4	11.8	11.9	17.5	17.5
$U4$	5.2	8.4	3.8	4.5	6.2	8.7	6.5	8.9	4.7	5.9	7.3	10.6	7.6	10.8	5.5	7.0	9.0	13.2	9.3	13.3
$U5$	6.9	14.8	6.9	7.8	7.3	8.4	8.7	9.6	8.4	9.8	8.7	10.3	10.6	11.9	10.4	12.0	10.8	12.8	13.2	14.7
$U6$	11.9	5.8	7.3	5.3	5.5	5.7	7.6	6.8	9.1	6.3	7.1	7.2	9.5	8.3	11.2	8.1	8.6	8.8	11.6	10.4
ED		0.94	1.41	1.74	1.81	1.52	1.88	1.83	1.84	2.29	2.36	1.96	2.44	2.38	2.18	2.70	2.81	2.34	2.90	2.83

Table 6: 95% CL exclusion limits on the contact interaction mass scales Λ^- and Λ^+, and on the the effective Plank scales M_S^- and M_S^+ in the large extra dimensions (ED) model (for negative and positive coupling signs respectively) expected from the measurement of high-Q^2 NC DIS cross-sections at THERA, for different running scenarios, as indicated in the table. Limits from the global analysis of existing data [1, 14, 9] are included for comparison.

For the model of large extra dimensions, THERA will improve existing limits in any configuration. This is because the graviton exchange contribution increases with the increasing center-of-mass energy. THERA-800 will be sensitive to the effective Plank scale M_S up to about 2.8 TeV.

In the limit of heavy leptoquark masses ($M_{LQ} \gg \sqrt{s}$) contact interaction model has been also used to set limits on the leptoquark mass to the coupling ratio M_{LQ}/λ_{LQ}. Expected 95% CL exclusion limits, for different leptoquark models and different THERA running scenarios are presented in Tab. 7. Current limits from the global analysis [2] are included for comparison. In most cases existing limits are already above THERA sensitivity, even in the highest electron energy option. Limits on M_{LQ}/λ_{LQ} can be only improved for $\tilde{V}_\circ$ and $\tilde{V}_{1/2}$ models.

For leptoquark masses comparable with the available center-of-mass energy, contact interaction approach has to be modified, as described in Sect. 3.3. Limits on λ_{LQ} are calculated as a function of the leptoquark mass M_{LQ} from the two-dimensional probability function $\mathcal{P}(\lambda_{LQ}, M_{LQ})$. For leptoquark masses smaller than the available center-of-mass energy ($M_{LQ} < \sqrt{s}$), limits are also set from the measurement of the direct leptoquark production. It turns out both approaches give similar results [2]. Measurement of the direct leptoquark production process results in better limits for low leptoquark masses ($M_{LQ} \ll \sqrt{s}$) and for leptoquark production involving valence quarks (production of F=2 leptoquarks in e^-p collisions or F=0 leptoquarks in e^+p collisions). $\frac{d\sigma}{dQ^2}$ measurement can results in slightly better limits (than expected from the direct production process) for leptoquark masses close to the center-of-mass energy and for leptoquark production from anti-quarks in the proton (F=0 leptoquarks in e^-p or F=2 in e^+p). For leptoquark masses $M_{LQ} < \sqrt{s}$ both kinds of limits are always calculated and the stronger one is taken.

Shown in Fig. 2, 3 and 4 are expected 95% CL exclusion limits in (λ_{LQ}, M_{LQ}), for different leptoquark models and THERA running with 250 GeV, 500 GeV and 800 GeV electron (positron) beam respectively. Limits expected from e^-p data and from e^+p data are compared. As expected, better limits on the F=2 leptoquark Yukawa coupling λ_{LQ}, for $M_{LQ} < \sqrt{s}$, are obtained from e^-p data, whereas e^+p data constrain better F=0 leptoquarks. Differences between limits expected from e^-p and e^+p data are smaller for scalar leptoquarks with $M_{LQ} > \sqrt{s}$. For high-mass vector leptoquarks it turns out that better limits can be obtained for "wrong" beam choice (e^-p for F=0 leptoquarks and e^+p for F=2 leptoquarks). Limits expected from combined e^-p and e^+p data, for different THERA running scenarios, are compared with existing limits [2] in Fig. 5. In all cases search for single leptoquark production at THERA significantly improves the existing limits.

In Fig. 6, 7, 8 and 9, limits on the leptoquark Yukawa coupling λ_{LQ} and mass M_{LQ} expected from THERA are compared with existing limits and limits expected from other future experiments [3], for $S^R_{1/2}$, S_1, $\tilde{V}_\circ$ and $V^L_{1/2}$ leptoquark models respectively.[4] Leptoquarks with masses up to about 2.0 TeV can be searched for at LHC, independently of

[4] Selected models were shown to describe the existing experimental data better than the Standard Model [2].

Model	Current limit [TeV]	Expected 95% CL exclusion limits on M_{LQ}/λ_{LQ} [TeV]								
		THERA-250			THERA-500			THERA-800		
		e^-p	e^+p	$e^\pm p$	e^-p	e^+p	$e^\pm p$	e^-p	e^+p	$e^\pm p$
$S_\circ^L$	3.7	1.7	1.2	1.7	2.1	1.5	2.2	2.5	1.8	2.7
$S_\circ^R$	3.9	1.5	1.1	1.5	1.8	1.4	1.9	2.2	1.6	2.4
$\tilde{S}_\circ$	3.6	0.7	0.6	0.7	0.9	0.8	0.9	1.1	0.9	1.1
$S_{1/2}^L$	3.5	0.6	1.0	1.0	0.8	1.2	1.2	0.9	1.5	1.5
$S_{1/2}^R$	2.1	0.7	1.0	1.0	0.9	1.3	1.3	1.0	1.6	1.6
$\tilde{S}_{1/2}$	3.8	0.6	1.0	1.0	0.8	1.2	1.2	1.0	1.5	1.5
S_1	2.4	1.4	1.0	1.4	1.7	1.2	1.7	2.1	1.5	2.1
$V_\circ^L$	8.1	1.6	1.4	1.8	2.1	1.8	2.3	2.5	2.2	2.8
$V_\circ^R$	2.3	1.3	1.1	1.4	1.7	1.4	1.8	2.0	1.7	2.1
$\tilde{V}_\circ$	1.9	1.8	1.2	1.9	2.1	1.6	2.4	2.7	1.9	2.9
$V_{1/2}^L$	2.1	0.8	1.1	1.1	1.0	1.4	1.4	1.2	1.7	1.7
$V_{1/2}^R$	7.5	1.2	2.0	2.0	1.5	2.5	2.5	1.8	3.0	3.1
$\tilde{V}_{1/2}$	2.1	1.1	2.0	2.1	1.4	2.5	2.5	1.6	3.1	3.1
V_1	7.3	2.6	1.5	2.8	3.1	1.9	3.3	3.9	2.3	4.2

Table 7: 95% CL exclusion limits on M_{LQ}/λ_{LQ} (in the limit of heavy leptoquark masses $M_{LQ} \gg \sqrt{s}$) expected from the measurement of high-Q^2 NC DIS cross-sections at THERA, for different running scenarios, as indicated in the table.

λ_{LQ}. THERA will not be able to improve any limits if LHC excludes leptoquark masses below 1.6 TeV. However, if any leptoquark type state is discovered at LHC, THERA will be the best place to study its properties, covering the widest range in (λ_{LQ}, M_{LQ}) space. Leptoquark mass, spin, fermion number and branching fraction (assuming leptoquark decays into $\nu + jet$ are reconstructed) can be determined. Yukawa coupling can be precisely measured down to the very small coupling values of the order of $\lambda_{LQ} \sim 10^{-2}$, not accessible at LHC.

6 Summary

The sensitivity of THERA to different contact interaction models has been studied in detail. For models conserving parity, scales up to about 18 TeV can be probed at THERA, extending considerably beyond the existing bounds. Significant improvement of existing limits is also expected for models with large extra dimensions. Effective Plank mass scales up to about 2.8 TeV can be probed. THERA will be the best machine to study leptoquark properties, for leptoquark masses up to about 1 TeV. It will be sensitive to the leptoquark Yukawa couplings down to $\lambda_{LQ} \sim 10^{-2}$.

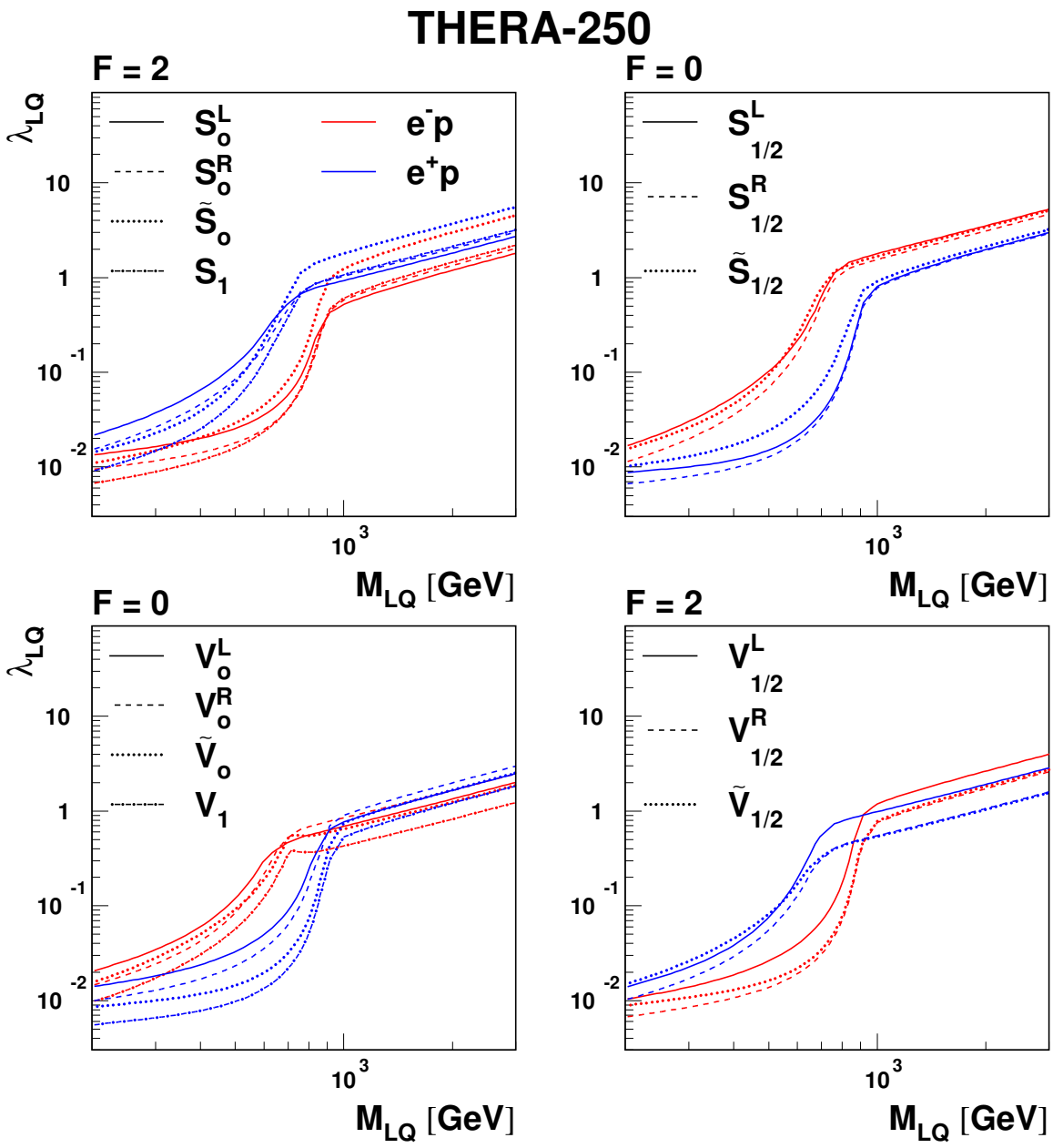

Figure 2: Expected 95% CL exclusion limits in (λ_{LQ}, M_{LQ}) space, for different leptoquark models (as indicated in the plot), for 100 pb^{-1} of e^-p data (red curves) and 100 pb^{-1} of e^+p data (blue curves) collected at 250 GeV electron (positron) beam energy (THERA-250). Limits based on single leptoquark production and high-Q^2 NC DIS cross-section measurements.

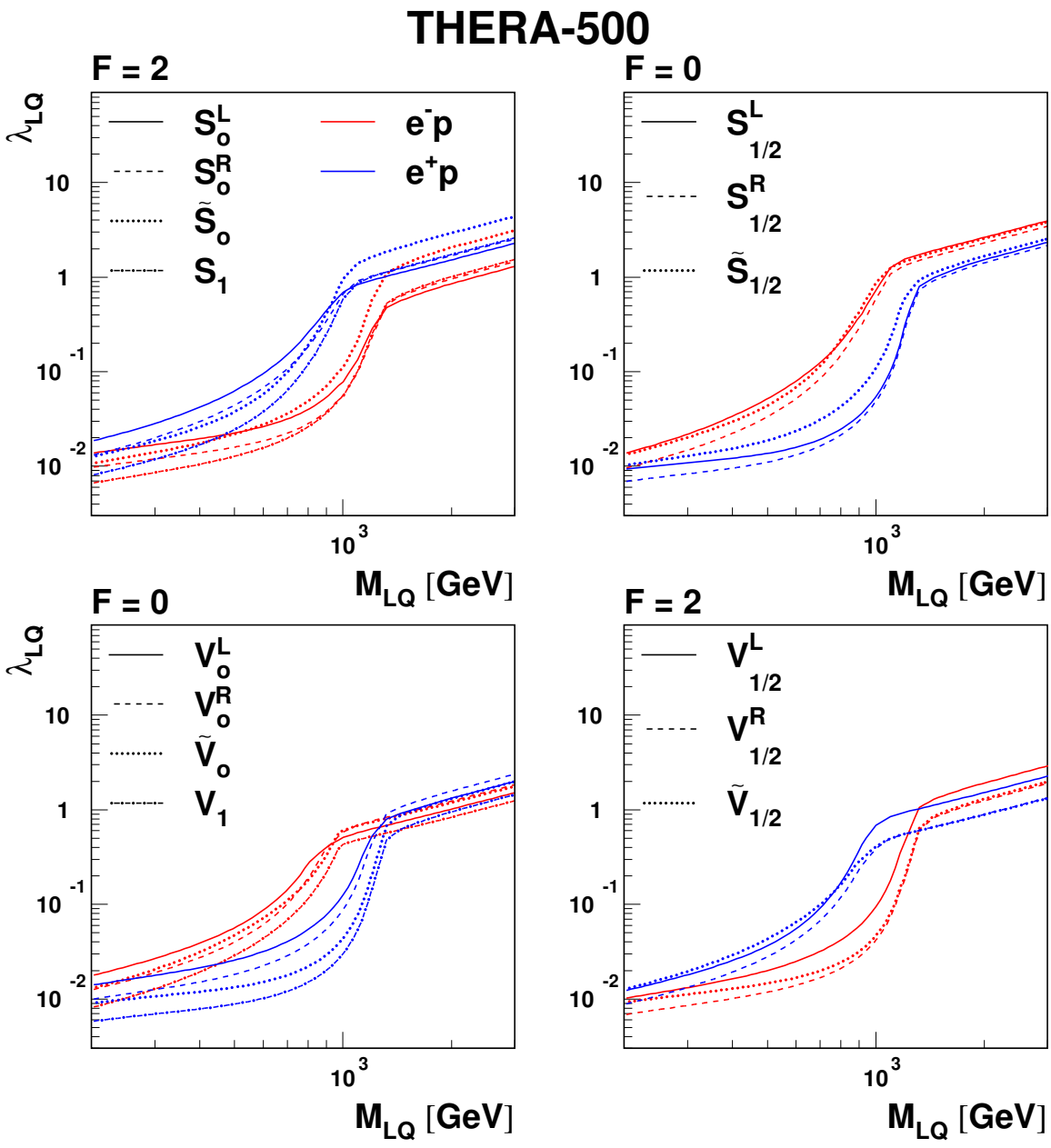

Figure 3: Expected 95% CL exclusion limits in (λ_{LQ}, M_{LQ}) space, for different leptoquark models (as indicated in the plot), for 100 pb^{-1} of e^-p data (red curves) and 100 pb^{-1} of e^+p data (blue curves) collected at 500 GeV electron (positron) beam energy (THERA-500). Limits based on single leptoquark production and high-Q^2 NC DIS cross-section measurements.

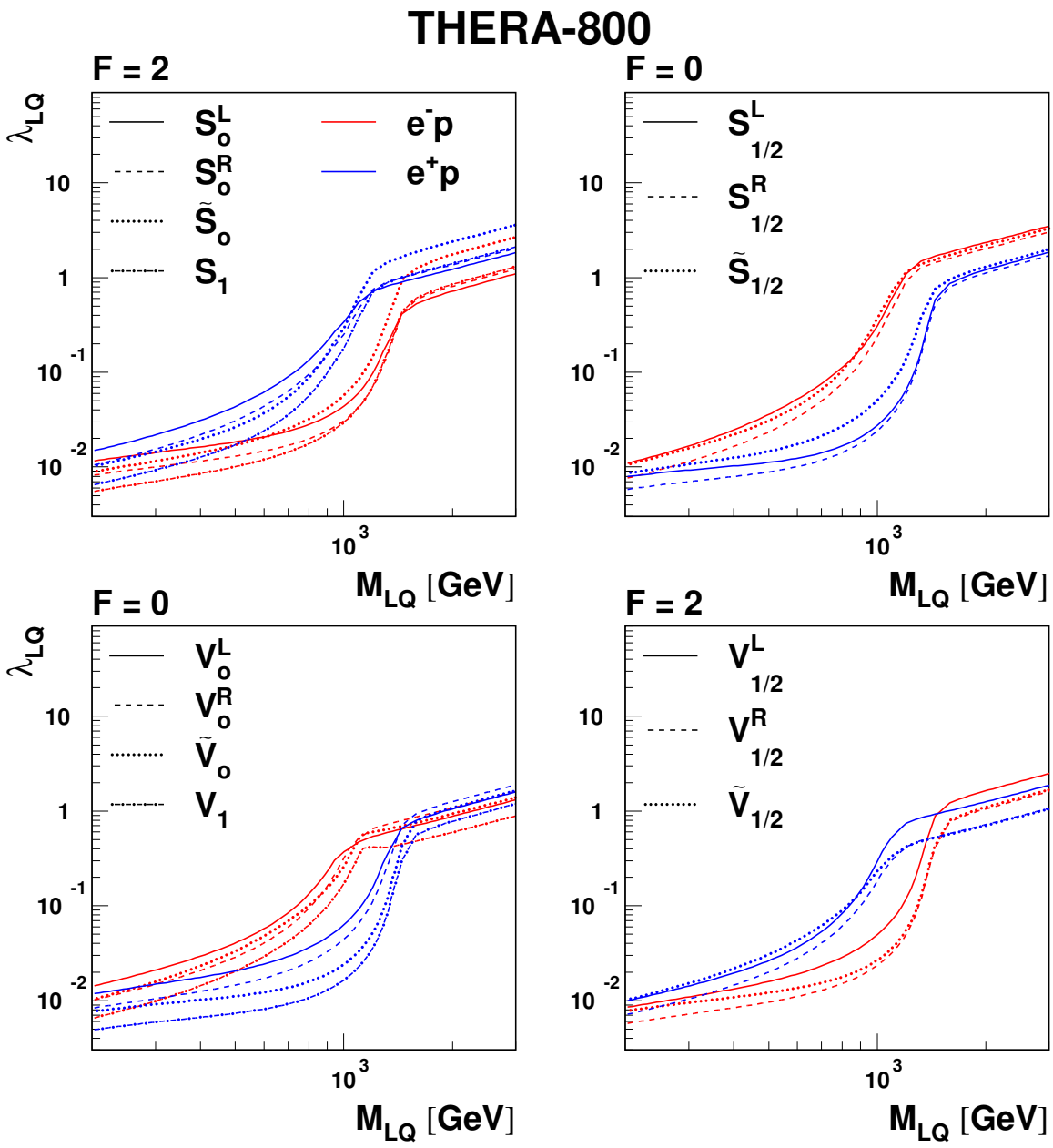

Figure 4: Expected 95% CL exclusion limits in (λ_{LQ}, M_{LQ}) space, for different leptoquark models (as indicated in the plot), for 200 pb^{-1} of e^-p data (red curves) and 200 pb^{-1} of e^+p data (blue curves) collected at 800 GeV electron (positron) beam energy (THERA-800). Limits based on single leptoquark production and high-Q^2 NC DIS cross-section measurements.

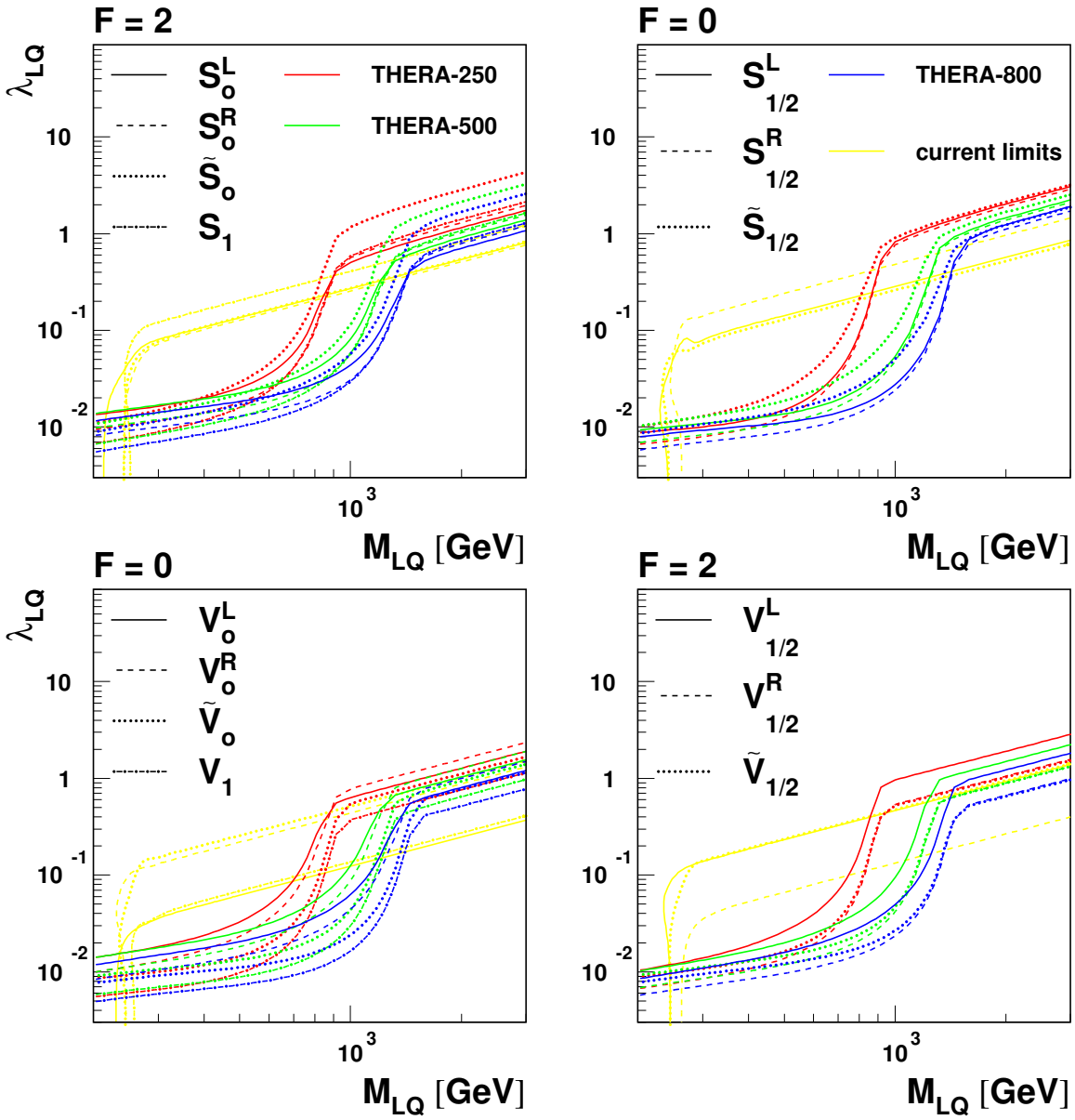

Figure 5: Expected 95% CL exclusion limits in (λ_{LQ}, M_{LQ}) space, for different leptoquark models and for different THERA running scenarios (as indicated in the plot). Limits based on single leptoquark production and high-Q^2 NC DIS cross-section measurements from the combined e^-p and e^+p data. Indicated in yellow are existing limits from global analysis [2].

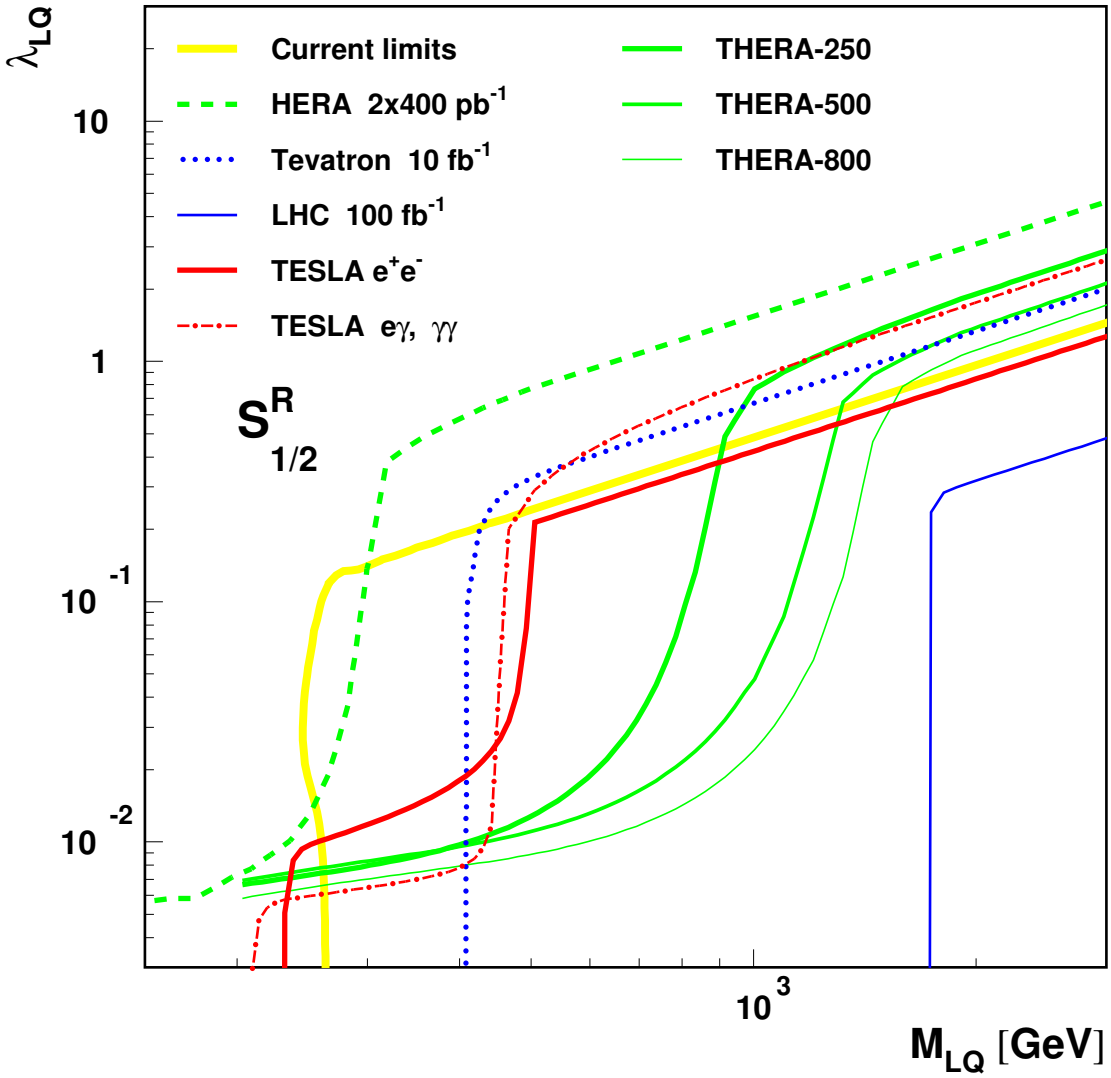

Figure 6: Comparison of expected 95% CL exclusion limits in (λ_{LQ}, M_{LQ}) for $S^R_{1/2}$ leptoquark model, for different THERA running scenarios and other future experiments, as indicated in the plot. Presented limits correspond to 2×400 pb^{-1} of $e^{\pm}p$ data at HERA ($\sqrt{s}$=318 GeV), 2×100 pb^{-1} or 2×200 pb^{-1} of $e^{\pm}p$ data at THERA ($\sqrt{s}$=1.0,1.4 and 1.6 TeV), 10 fb^{-1} of $p\bar{p}$ data at the Tevatron ($\sqrt{s}$=2 TeV), 100 fb^{-1} of pp data at the LHC ($\sqrt{s}$=14 TeV) and 100 fb^{-1} of e^+e^-, $e\gamma$ and $\gamma\gamma$ data at TESLA ($\sqrt{s_{ee}}$=500 GeV). Also indicated are 95% CL exclusion limits from global analysis of existing data[2].

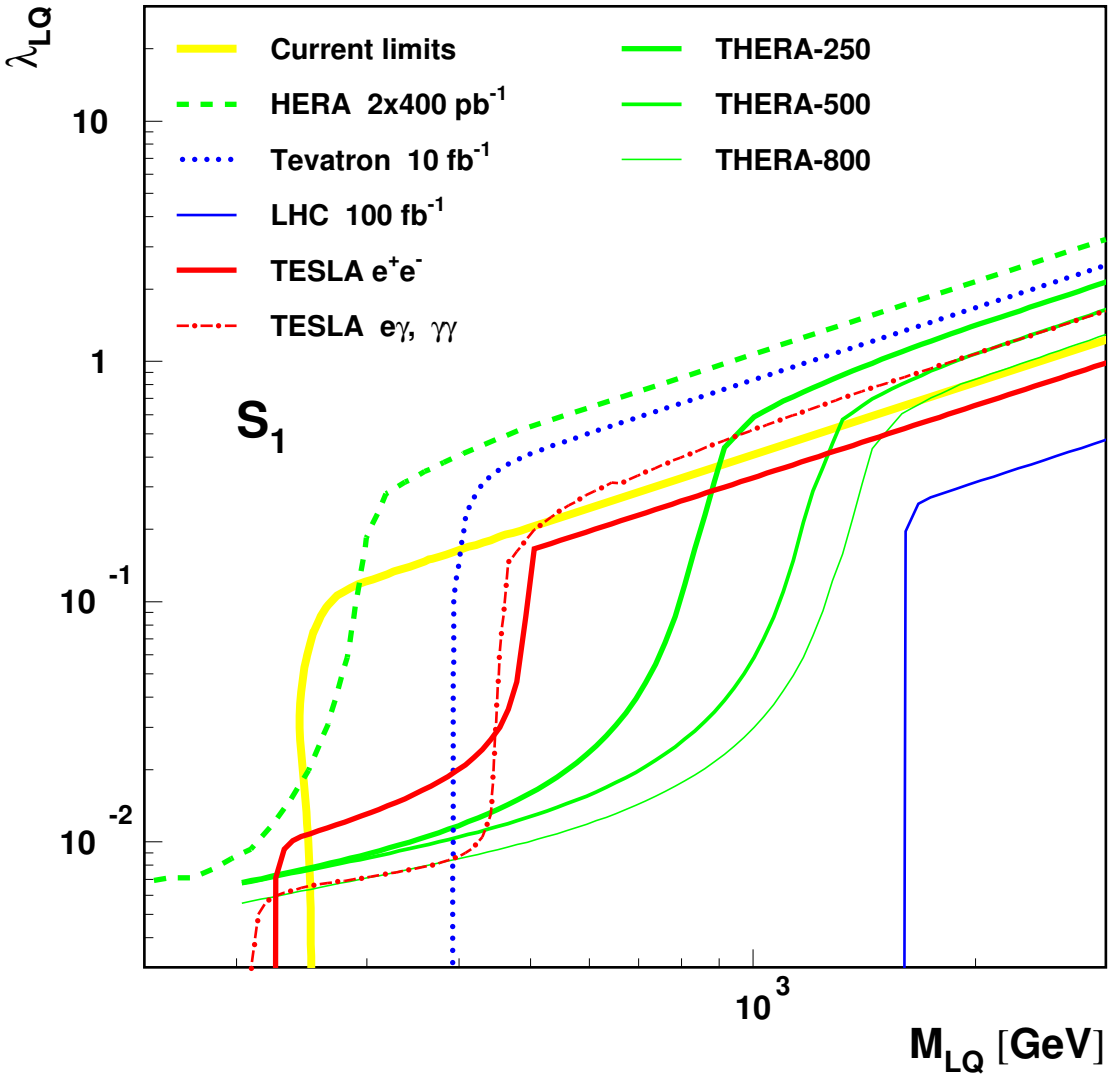

Figure 7: Comparison of expected 95% CL exclusion limits in (λ_{LQ}, M_{LQ}) for S_1 leptoquark model, for different THERA running scenarios and other future experiments, as indicated in the plot. Presented limits correspond to 2×400 pb^{-1} of $e^{\pm}p$ data at HERA ($\sqrt{s}$=318 GeV), 2×100 pb^{-1} or 2×200 pb^{-1} of $e^{\pm}p$ data at THERA ($\sqrt{s}$=1.0,1.4 and 1.6 TeV), 10 fb^{-1} of $p\bar{p}$ data at the Tevatron ($\sqrt{s}$=2 TeV), 100 fb^{-1} of pp data at the LHC ($\sqrt{s}$=14 TeV) and 100 fb^{-1} of e^+e^-, $e\gamma$ and $\gamma\gamma$ data at TESLA ($\sqrt{s_{ee}}$=500 GeV). Also indicated are 95% CL exclusion limits from global analysis of existing data[2].

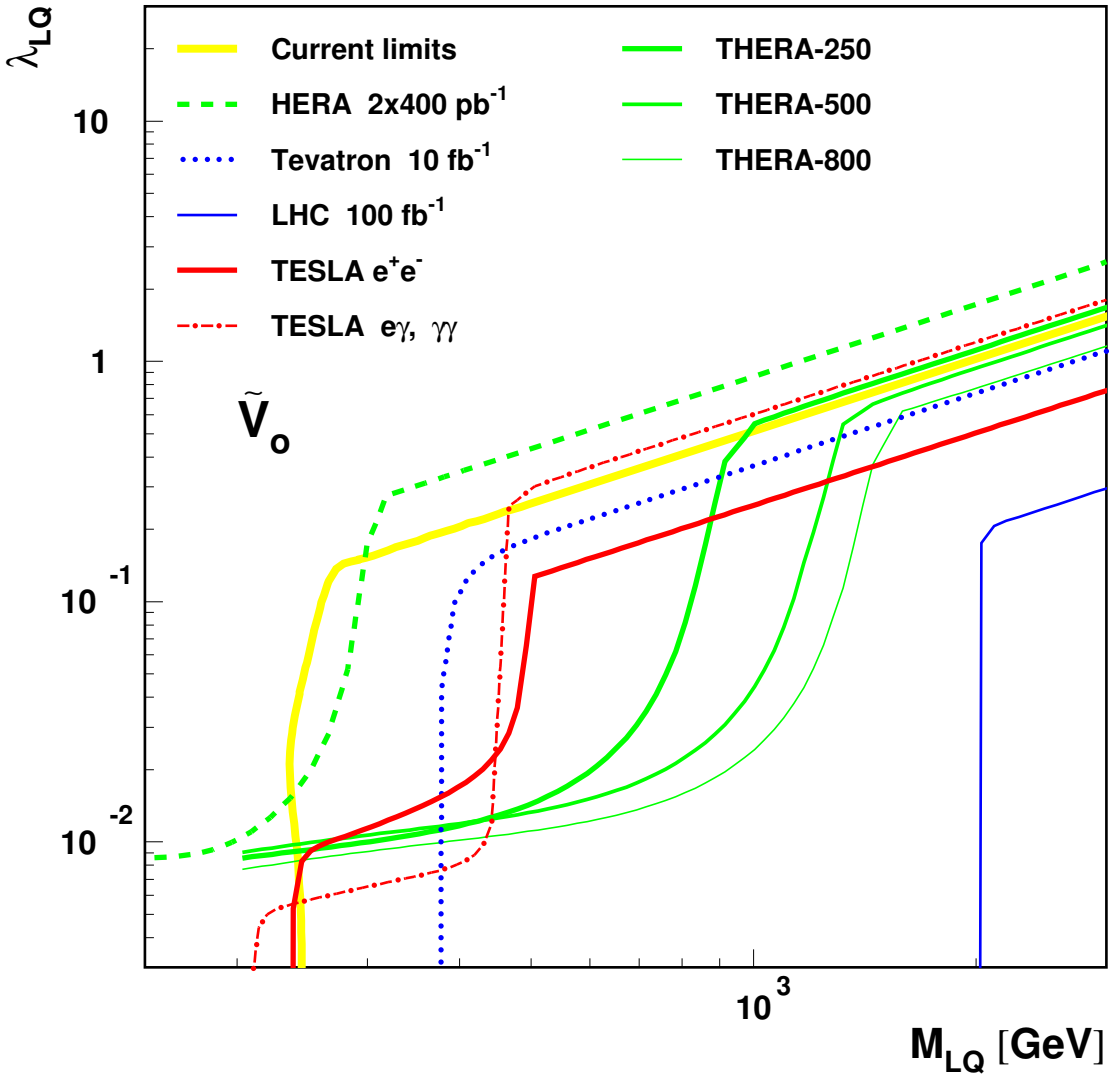

Figure 8: Comparison of expected 95% CL exclusion limits in (λ_{LQ}, M_{LQ}) for $\tilde{V}_\circ$ leptoquark model, for different THERA running scenarios and other future experiments, as indicated in the plot. Presented limits correspond to 2×400 pb^{-1} of $e^{\pm}p$ data at HERA ($\sqrt{s}$=318 GeV), 2×100 pb^{-1} or 2×200 pb^{-1} of $e^{\pm}p$ data at THERA ($\sqrt{s}$=1.0,1.4 and 1.6 TeV), 10 fb^{-1} of $p\bar{p}$ data at the Tevatron ($\sqrt{s}$=2 TeV), 100 fb^{-1} of pp data at the LHC ($\sqrt{s}$=14 TeV) and 100 fb^{-1} of e^+e^-, $e\gamma$ and $\gamma\gamma$ data at TESLA ($\sqrt{s_{ee}}$=500 GeV). Also indicated are 95% CL exclusion limits from global analysis of existing data[2].

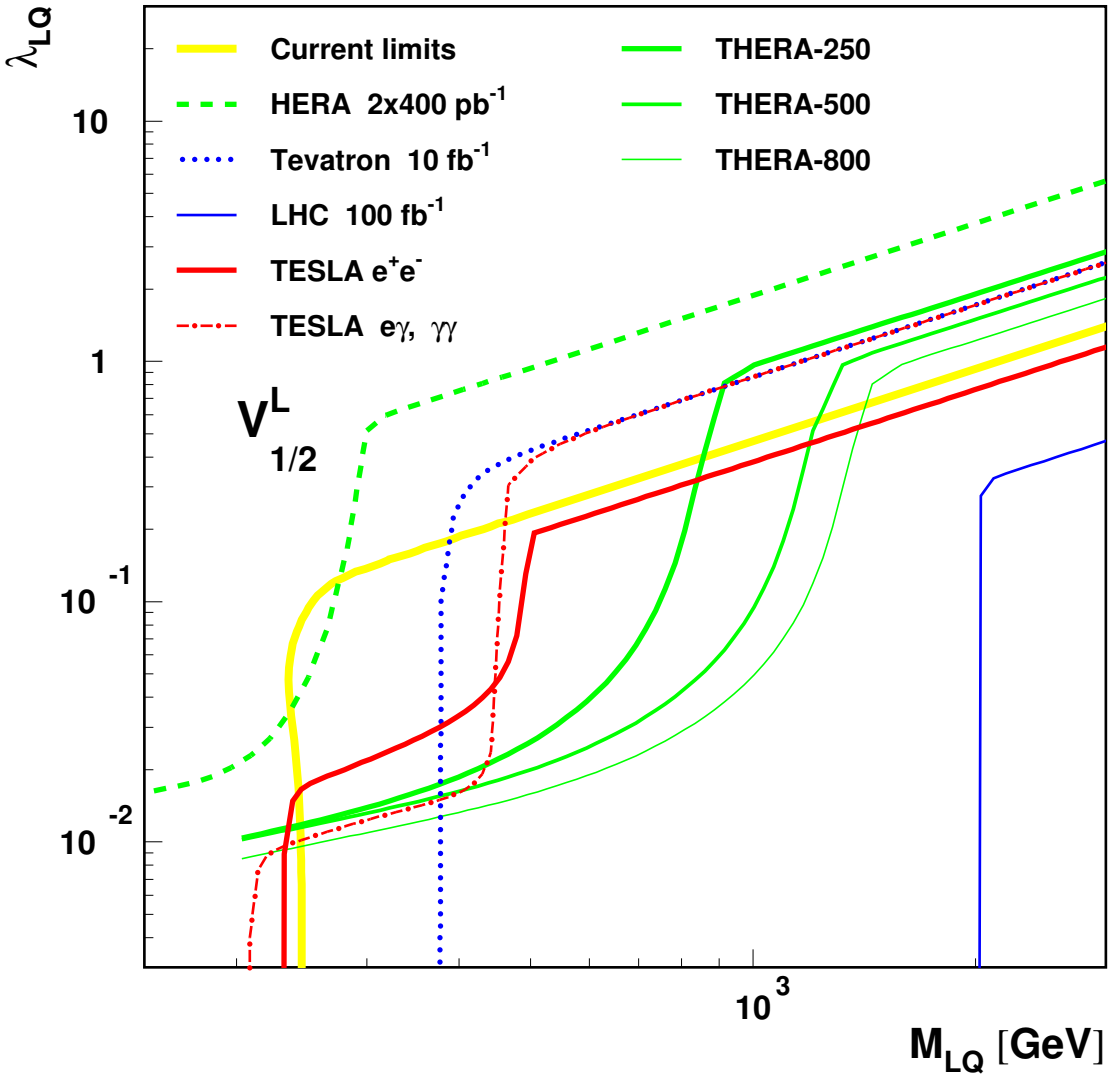

Figure 9: Comparison of expected 95% CL exclusion limits in (λ_{LQ}, M_{LQ}) for $V^L_{1/2}$ leptoquark model, for different THERA running scenarios and other future experiments, as indicated in the plot. Presented limits correspond to 2×400 pb^{-1} of $e^{\pm}p$ data at HERA ($\sqrt{s}$=318 GeV), 2×100 pb^{-1} or 2×200 pb^{-1} of $e^{\pm}p$ data at THERA ($\sqrt{s}$=1.0,1.4 and 1.6 TeV), 10 fb^{-1} of $p\bar{p}$ data at the Tevatron ($\sqrt{s}$=2 TeV), 100 fb^{-1} of pp data at the LHC ($\sqrt{s}$=14 TeV) and 100 fb^{-1} of e^+e^-, $e\gamma$ and $\gamma\gamma$ data at TESLA ($\sqrt{s_{ee}}$=500 GeV). Also indicated are 95% CL exclusion limits from global analysis of existing data[2].

References

[1] A. Żarnecki, Eur. Phys. J. **C11**, 539 (1999).

[2] A. Żarnecki, Eur. Phys. J. **C17**, 695 (2000).

[3] A. Żarnecki, hep-ph/0006335, subm. to *ICHEP2000, Osaka*, abstract 193.

[4] P. Haberl, F. Schrempp and H.U. Martyn, in *Proc. Physics at HERA, vol. 2*, edited by W. Buchmüller and G. Ingelman (DESY, Hamburg, Germany, 1991), p. 1133.

[5] V. Barger, K. Cheung, K. Hagiwara and D. Zeppenfeld, Phys. Rev. **D57**, 391 (1998).

[6] D. Zeppenfeld and K. Cheung, hep-ph/9810277.

[7] N. Arkani-Hamed, S. Dimopoulos and G. Dvali, Phys. Lett. **B429**, 263 (1998).

[8] N. Arkani-Hamed, S. Dimopoulos and G. Dvali, Phys. Rev. **D59**, 086004 (1999).

[9] K. Cheung, Phys. Lett. **B460**, 383 (1999).

[10] W. Buchmüller, R. Rückl and D. Wyler, Phys. Lett. **B191**, 442 (1987), erratum in Phys. Lett. **B 448** 320 (1999).

[11] W. Buchmüller and D. Wyler, Phys. Lett. **B177**, 377 (1986).

[12] A. Djouadi, T. Kohler, M. Spira and J. Tutas, Z. Phys. **C46**, 679 (1990).

[13] J. Kalinowski, R. Rückl, H. Spiesberger and P.M. Zerwas, Z. Phys. **C74**, 595 (1997).

[14] A. Żarnecki, hep-ph/0006196, contrib. to *DIS2000*, Liverpool.

[15] C. Wood *et al.*, Science **275**, 1759 (1997).

[16] S.A. Blundell, J. Sapirstein and W.R. Johnson, Phys. Rev. **D45**, 1602 (1992).

[17] S.C. Bennett and C.E. Wieman, Phys. Rev. Lett. **82**, 2484 (1999).